

## **Controlled Source Electromagnetic Interferometry by multidimensional deconvolution: spatial sampling aspects in Sea Bed Logging**

Jürg Hunziker, Evert Slob, Kees Wapenaar

### **summary**

We review electromagnetic interferometry by multidimensional deconvolution (MDD) and investigate its sensitivity to spatial sampling. Two Sea Bed Logging datasets were modeled numerically. One represents a shallow sea situation with a small vertical source receiver distance and the other a deep sea situation with a large vertical source receiver distance. The reflection response from below the receivers was retrieved by interferometry by MDD after decomposition of the field into up- and downgoing fields. This reflection response is independent of any effects of the water layer and consequently the same for both situations. It could be shown, that for a shallow sea situation a denser sampling is necessary than for a deep sea situation to decompose the fields and apply MDD successfully.



## Introduction

In seismics, interferometry is well known as the process of cross-correlating two traces at two receiver positions to retrieve the Green's function between these two receivers. The theory has been derived and applied for controlled-source and passive cases by various authors. Wapenaar et al. (2008a) and Schuster (2009) give a comprehensive overview. Interferometry by cross-correlation has also been derived for electromagnetics (Slob et al. 2007).

It has been shown that the process of cross-correlation (CC) can be replaced by a multi-dimensional deconvolution (MDD) in the controlled-source case (Wapenaar et al. 2008b) and in the passive case (Wapenaar et al. 2008c). The advantages of MDD include elimination of the source signature, improved radiation characteristics of the retrieved source and relaxation of the assumption of a lossless medium. On the other hand MDD is more expensive and the matrix inversion involved may be unstable. Furthermore a decomposition of the measured fields into up- and downgoing fields is necessary.

In this paper Controlled Source Electromagnetic (CSEM) data in a marine environment is considered. This is often referred to as Sea Bed Logging (SBL), where an electric-dipole source is towed behind a boat emitting a low-frequency electric field, which propagates through the subsurface and through the water. The resulting EM-field is recorded at the ocean bottom by horizontal multicomponent receivers as a function of offset. At small source/receiver offsets the field is dominated by the direct field and reflections from the sea surface. At large offsets the refraction from the sea surface (airwave) is very strong (Amundsen et al. 2006). Consequently the recorded signal depends on the thickness of the water layer.

By applying interferometry by MDD the source is redatumed to the receiver level, the direct field is eliminated and the water layer is replaced by a homogenous overburden. In other words, all effects of the water layer, including the dependence on its thickness, are removed. In this paper the necessary receiver spacing for a successful decomposition and subsequent MDD is investigated for a deep and a shallow sea configuration using numerical examples.

## Theory

The multicomponent electromagnetic fields are decomposed into up- and downgoing fields  $\hat{P}^-(x_R, x_S)$  and  $\hat{P}^+(x_R, x_S)$  respectively using an algorithm derived by Slob (to appear in IEEE-TGRS, 2009). The receiver coordinates are represented by  $x_R$  and the source coordinates by  $x_S$ . The decomposition can be done at any depth level where no sources are present. The implementation used here assumes the material parameters to be laterally constant at the depth level of decomposition. The decomposed fields are related to each other through the reflection response  $\hat{R}_0^+(x_R, x'_R)$

$$\hat{P}^-(x_R, x_S) = \int_{\partial D_R} \hat{R}_0^+(x_R, x'_R) \hat{P}^+(x'_R, x_S) dx'_R, \quad (1)$$

where the integration is taken over all receivers and the circumflex denotes space-frequency domain. The superscript  $^+$  in the reflection response indicates that its origin is a downgoing field and the subscript  $_0$  represents the absence of heterogeneities above the receiver level. This equation can be rewritten in matrix notation (Berkhout 1982) as

$$\hat{P}^- = \hat{R}_0^+ \hat{P}^+. \quad (2)$$

Interferometry by MDD solves equation 2 for  $\hat{R}_0^+$  in a least-squares sense

$$\hat{R}_0^+ = \hat{P}^- (\hat{P}^+)^{\dagger} \left[ \hat{P}^+ (\hat{P}^+)^{\dagger} + \varepsilon^2 \mathbf{I} \right]^{-1}. \quad (3)$$

The superscript  $^{\dagger}$  denotes complex-conjugation and transposition and  $\mathbf{I}$  is the identity matrix. The stabilisation parameter  $\varepsilon$  prevents the inversion from getting unstable. The retrieved  $\hat{R}_0^+$  is the field with a source at the receiver level, without a direct field and with the water layer replaced with a halfspace consisting of the same material as the first layer below the water.

### Modeling and Processing

Two 2D Transverse Magnetic SBL-datasets are modeled in the wavenumber domain. Consequently there is a  $J_x$  source at a frequency of 0.5 Hz and  $E_x$  and  $H_y$  receivers, where  $J$  stands for an electric source whose antenna orientation is given by the subscript. The electric and magnetic field components are represented with  $E$  and  $H$  respectively. Their receiver component is indicated by the subscript. The datasets are obtained in a configuration that consists from top to bottom of a halfspace of air, a water layer and halfspace of ground. The latter is intersected by a reservoir layer. The difference between the two datasets is the thickness of the water layer  $h$ , which is 200 m in one case to simulate a shallow sea environment and 1000 m in the other case, standing for a deep sea situation. The source is located 175 m below the sea surface. Consequently the vertical source receiver distance  $z_{sr}$  is 25 m for the shallow sea situation and 825 m for the deep sea situation. All the electrical and geometrical parameters are given in figure 1 a).

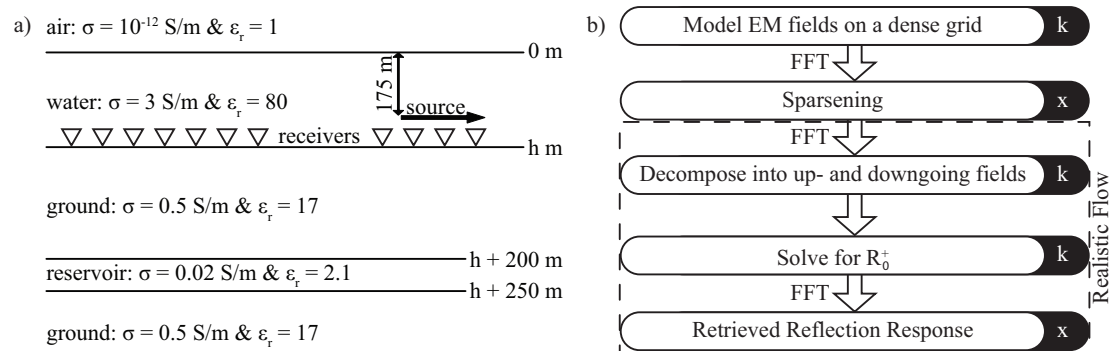


Figure 1: a) Setup of numerical modeling: The black arrow indicates the source, white triangles the receivers. Conductivity  $\sigma$  and relative permittivity  $\epsilon_r$  are given in the according layer. b) Processing flow: The dashed box labeled Realistic Flow contains all the steps that would be applied to a real dataset. The letters x and k on black ground indicate space and wavenumber domain respectively.

Next the datasets are inverse Fourier transformed to space domain, where samples are deleted to create more sparse datasets. Then the datasets are decomposed into up- and downgoing fields in the wavenumber domain. Since the medium is laterally invariant, equation 3 can be solved fast in wavenumber domain, where MDD becomes a simple division. The inverse Fourier transformed result is equivalent with the  $\hat{R}_0^+$  retrieved by MDD. The complete processing flow is shown in figure 1 b).

### Results

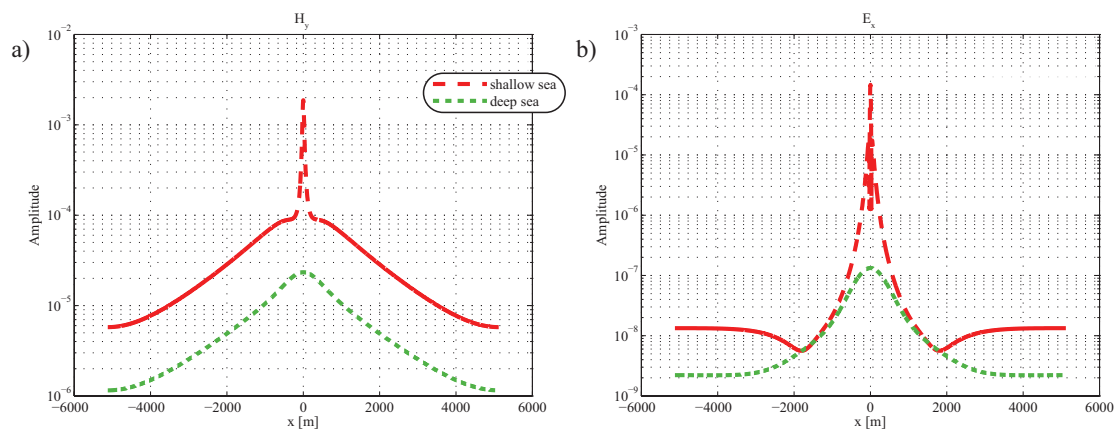


Figure 2: Electromagnetic fields in the space domain as a function of offset for the shallow sea (red dashed line) and the deep sea (green denser dashed line) situation on a semi logarithmic plot. a)  $H_y$  b)  $E_x$ . (Note that the horizontal tails of the curves at large offsets have not a physical origin, but stem from the Fourier Transformation.)

The magnitude of the two electromagnetic field components  $H_y$  and  $E_x$  are shown in figure 2 in a semi logarithmic plot. The shallow sea situation is plotted with a red dashed line and the deep sea situation with a green denser dashed line. Note that in the deep sea situation the source is vertically further away from the receivers than in the shallow sea situation. Therefore the slope of the curve representing the shallow sea case is steeper at small offsets for both field components than in the deep sea case. In wavenumber domain this corresponds to energy at higher wavenumbers in the shallow sea situation than in the deep sea situation.

The reflection response  $\hat{\mathbf{R}}_0^+$ , which is retrieved after decomposition into up- and downgoing fields and MDD, is shown in figure 3 for the shallow sea (red dashed line) and the deep sea situation (green denser dashed line) as a function of offset for different spacings  $dx$ . The total offset is kept constant, therefore with increasing spacing  $dx$  the number of samples  $N$  decreases. Since MDD replaces the water layer with a halfspace, the reflection responses for the shallow sea and the deep sea situation should be identical (in case of correct sampling). The retrieved reflection responses are compared with a directly modeled reflection response (black solid line).

In figure 3 a) the spacing  $dx$  is equal to 2.5 m. Both retrieved reflection responses and the directly modeled reflection response show exactly the same shape verifying that MDD was applied successfully and the effect of the water layer is removed for both cases. This is different in figure 3 b) where the retrieved reflection response for the shallow sea shows some artifacts at very small offsets. As seen in figure 2 and mentioned earlier, the electromagnetic fields decay faster in space in the shallow sea situation. Increasing the spacing introduces aliasing for the high wavenumbers in the wavenumber domain and therefore affects the decomposition algorithm. Improperly decomposed fields lead to artifacts in the retrieved reflection response. A sampling of  $dx = 5$  m seems already to be too large. For the deep sea situation, the fields decay less strong and therefore this sampling is still sufficient. To detect reservoirs in the subsurface, the small offsets are not of interest, and therefore the artifacts in this region can be ignored. When the spacing is further increased to  $dx = 40$  m as shown in figure 3 c), the reflection response for the shallow sea situation is now also for intermediate offsets not retrieved correctly. On the other hand for the deep sea situation  $\hat{\mathbf{R}}_0^+$  could be retrieved perfectly. Further increase of the spacing decreases the quality of  $\hat{\mathbf{R}}_0^+$  for the shallow sea situation as expected even more. With a spacing of  $dx = 160$  m also  $\hat{\mathbf{R}}_0^+$  for the deep sea gets slightly deteriorated. This becomes more pronounced for spacings like  $dx = 320$  m and  $dx = 640$  m as shown in figure 3 d).

Finally, an empirical rule of thumb for the maximum spacing  $dx$  as a function of the vertical source receiver distance  $z_{sr}$  can be set up. To retrieve the reflection response perfectly, sampling should be chosen such that  $dx \leq z_{sr}/10$ . If small artifacts around zero offset on  $\hat{\mathbf{R}}_0^+$  can be ignored, sampling is sufficient if  $dx \leq z_{sr}/5$ . These rather conservative rules have been tested for a frequency range from 0.25 Hz up to 2 Hz.

## Conclusions

SBL data were modeled for a shallow sea and a deep sea situation. The electromagnetic fields were decomposed and the reflection response  $\hat{\mathbf{R}}_0^+$  was retrieved with interferometry by MDD. Although the original electromagnetic fields are strongly affected by the thickness of the water layer,  $\hat{\mathbf{R}}_0^+$  is independent of it. Due to the fact that the original electromagnetic fields decay faster in the shallow sea situation than in the deep sea situation, because the source is closer to the receivers, a denser sampling is necessary. This is crucial in the wavenumber domain, because a too large sampling introduces aliasing for the high wavenumbers, leading to artifacts in the retrieved reflection response. A rule of thumb which relates vertical source receiver distance to the spatial sampling was presented.

## Acknowledgment

This research is supported by the Dutch Technology Foundation STW, applied science division of NWO and the Technology Program of the Ministry of Economic Affairs.

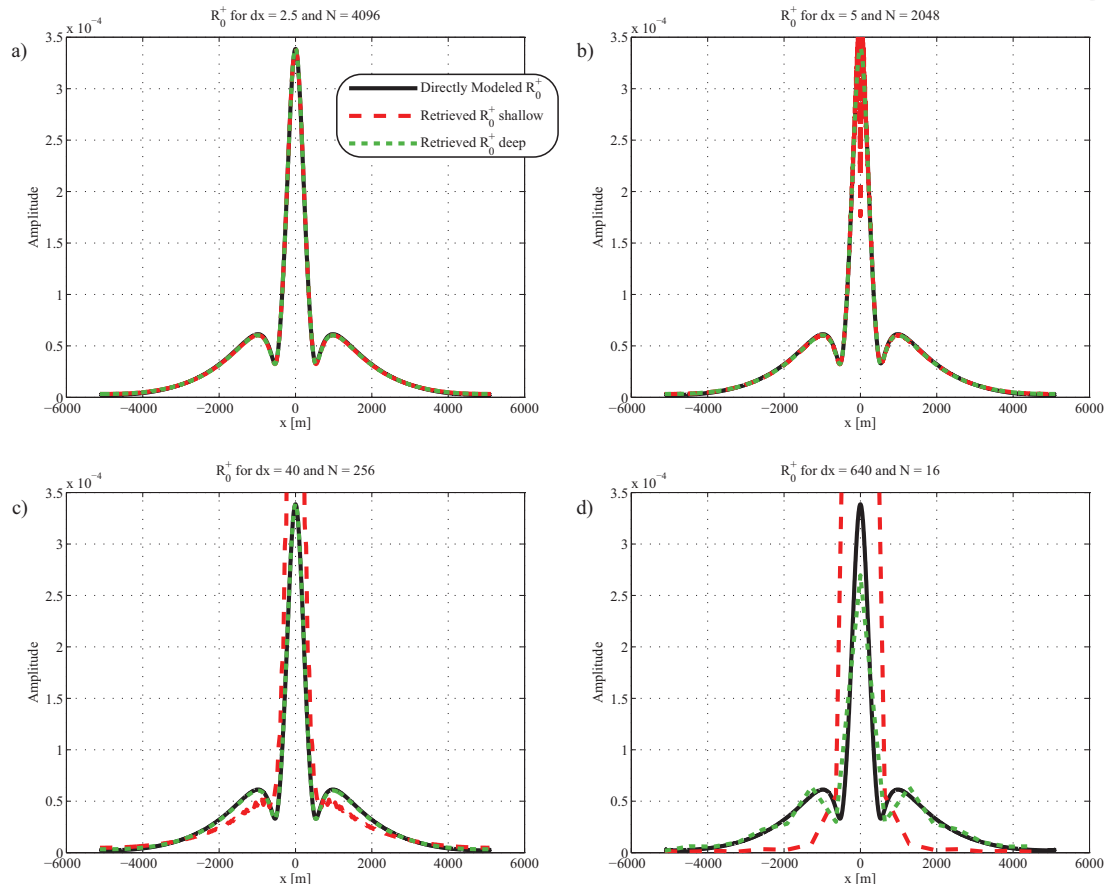


Figure 3: Reflection Responses for different spacings as a function of offset. Spacing  $dx$  and the amount of datapoints  $N$  is given in the figure captions. The spatial sampling  $dx$  is given in meters.

## References

- Amundsen, L., Løseth, L., Mittet, R., Ellingsrud, S. and Ursin, B. [2006] Decomposition of electromagnetic fields into upgoing and downgoing components. *Geophysics*, **71**(5), G211-G223.
- Berkhout, A. J. [1982] *Seismic Migration. Imaging of Acoustic Energy by Wave Field Extrapolation*. Elsevier
- Schuster, G. [2009] *Seismic Interferometry*. Cambridge University Press
- Slob, E., Draganov, D. and Wapenaar, K. [2007] Interferometric electromagnetic Green's functions representations using propagation invariants. *Geophysical Journal International*, **169**, 60-80.
- Wapenaar, K., Draganov, D. and Robertsson, J. O. A. [2008a] *Seismic interferometry: history and present status*. Society of Exploration Geophysicists, Geophysics Reprint Series No. 26.
- Wapenaar, K., Slob, E. and Snieder, R. [2008b] Seismic and electromagnetic controlled-source interferometry in dissipative media. *Geophysical Prospecting*, **56**, 419-434.
- Wapenaar, K., van der Neut, J. and Ruigrok, E. [2008c] Passive seismic interferometry by multidimensional deconvolution *Geophysics*, **73**, A51-A56